06

Application of cellulose paper with controlled electromagnetic characteristics as an interface in microwave photonic crystal

© A.V. Skripal, D.V. Ponomarev, M.A. Volshanik

Saratov National Research State University, Saratov, Russia
E-mail: skripala_v@info.sgu.ru

Received April 17, 2025
Revised July 18, 2025
Accepted August 12, 2025

Cellulose paper with controlled electromagnetic characteristics has been used as an interface for microwave photonic crystal. The change in the interface structure, as the introduction of an air gap, at certain values of the cellulose paper layer thickness and the mass fraction of distilled water leads to low frequency shift of the Tamm resonance, while the changes in the resonance amplitudes in the first forbidden band are monotonic, and in the second — non-monotonic.

Keywords: microwave absorbers, photonic Tamm resonances, cellulose, water.

DOI: 10.61011/TPL.2025.11.62210.20348

The interest in potential application of polymer porous composites [1,2] with conductive nanoinclusions, such as graphene [3,4], carbon nanotubes [5,6], and silver nanowires [7], in microwave technology for shielding and absorbing electromagnetic energy has been on the rise in recent years. Structures based on cellulose and its derivatives [8] with carbon nanotubes and silver nanowire inclusions [9–12] have also been proposed as an efficient, renewable, and environmentally friendly material for electromagnetic interference shielding. However, the fabrication of such materials with a uniform distribution of nanoinclusions still remains one of the key technological challenges.

Another trend in the design of environmentally friendly microwave absorbers of electromagnetic energy is the use of structures containing polar liquids (e.g., water) in the form of both continuous layers and individual periodically arranged droplets [13,14].

A structure made up of individual droplets with their electrical size (even with high values of permittivity taken into account) being significantly smaller than the wavelength of electromagnetic radiation is a composite surface characterized by an effective complex permittivity. The electromagnetic parameters of this surface may be controlled by adjusting the size of droplets and their packing density on a dielectric substrate [14]. However, the droplet size cannot be arbitrary and is largely determined by the properties of the substrate, such as the degree of its wetting by the liquid used.

An alternative option for an environmentally friendly absorber with its electromagnetic characteristics adjustable within a wide range is an absorber based on cellulose paper, which acts as a matrix that contains polar liquid (e.g., distilled water).

In the present paper, we report the results of application of cellulose paper with varying mass fractions of polar liquid (distilled water) as an interface in a study aimed at characterizing the effect of emergence of Tamm resonances in the bandgap of a photonic crystal within the microwave frequency range [15,16].

A model of a microwave photonic crystal based on a rectangular waveguide with dielectric filling consisting of Al_2O_3 ceramic layers and Teflon [16] was examined within the frequency range of 7–13 GHz.

A waveguide section filled with an electromagnetic energy absorber in the form of a layer of cellulose paper with varying mass fraction X of polar liquid (distilled water) and thickness d was adjacent to the photonic crystal. The layer of cellulose paper was bordered on both sides by Teflon films ($\varepsilon = 2.0$) with a thickness of 30 μm. An air gap was also created between the film and the last photonic crystal layer; width L of this gap was adjustable.

To ensure the accuracy of calculation of the frequency dependences of reflection $S_{11}(f)$ and transmission $S_{12}(f)$ coefficients of the photonic crystal by the transfer-matrix method [17–19], we used experimental values of the real (Fig. 1, *a*) and imaginary (Fig. 1, *b*) parts of complex permittivity $\varepsilon^*(f)$ of the cellulose paper layer within the frequency range of 7–13 GHz at various mass fractions X of polar liquid (distilled water). An Agilent N5242A vector network analyzer and the Agilent 85071E Materials Measurement Software were used to measure frequency dependence $\varepsilon^*(f)$ [20].

The use of cellulose paper with varying mass fractions of polar liquid (distilled water) as the interface leads to the emergence of Tamm resonances in the first and second bandgaps at frequencies f_{Tamm1} and f_{Tamm2}.

The positioning of resonances in the bandgaps is specified both by the geometric dimensions and electromagnetic characteristics of cellulose paper, which depend on the mass fraction of polar liquid, and by its position relative to the photonic crystal.

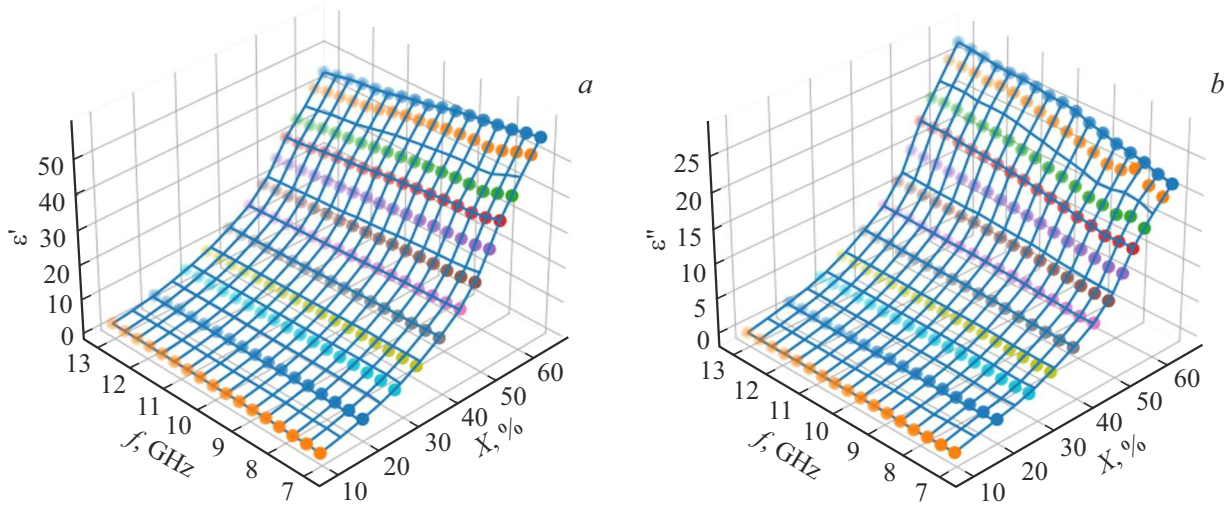

Figure 1. Experimental values of real $\varepsilon'(f)$ (a) and imaginary $\varepsilon''(f)$ (b) parts of complex permittivity $\varepsilon^*(f)$ of a cellulose paper layer at different mass fractions X of distilled water.

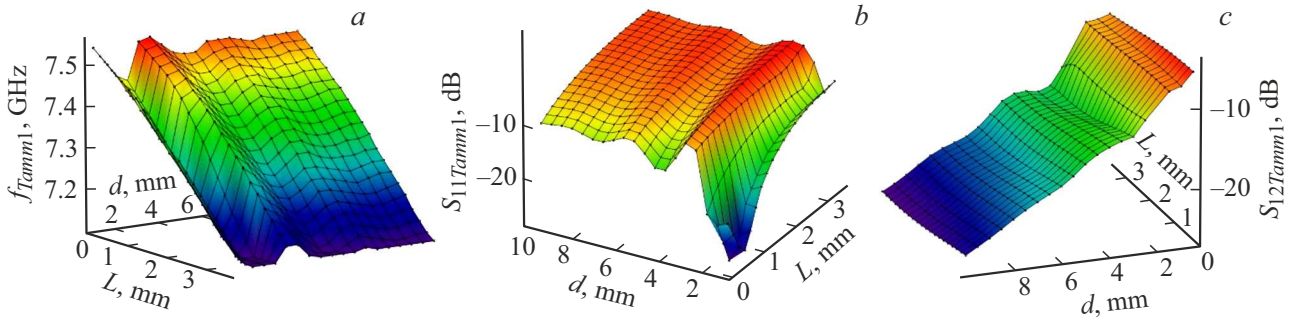

Figure 2. Calculated 3D maps of frequencies f_{Tamm1} (a) and amplitudes of reflection $S_{11Tamm1}$ (b) and transmission $S_{12Tamm1}$ (c) coefficients for the Tamm resonance in the first bandgap as functions of cellulose paper thickness d and air gap thickness L at a fixed mass content of water $X = 55\,\%$ in the material.

Figure 2 presents the calculation results in the form of 3D maps of frequencies f_{Tamm1} and amplitudes of reflection $S_{11Tamm1}$ and transmission $S_{12Tamm1}$ coefficients for the Tamm resonance in the first bandgap.

As the thickness of cellulose paper (with a mass fraction of polar liquid of 55 %) increases, damped oscillations of frequencies f_{Tamm1} and f_{Tamm2} of the Tamm resonances in the first (Fig. 2, a) and second bandgaps are observed. However, the frequency of oscillations in the first bandgap is significantly lower than in the second one.

An increase in thickness of cellulose paper also leads to damped oscillations of the reflection coefficient; at large thickness values, it assumes a constant magnitude that depends both on the mass fraction of water and on the gap between the last layer of the photonic crystal and the layer of cellulose paper (Fig. 2, b). In contrast to the dependence of the reflection coefficient, the dependence of the transmission coefficient on thickness of the cellulose paper layer is a monotonically decreasing function characterized by a non-monotonically varying rate of change at small thicknesses (Fig. 2, c). In the second bandgap, the transmission coefficient also decreases monotonically, but at a higher rate.

With a wider air gap L between the cellulose paper layer and the last layer of the photonic crystal, the Tamm resonance shifts lower in frequency in both the first and second bandgaps. The frequency shift in the second bandgap from its high-frequency edge to the low-frequency one is as large as 1.3 GHz, which is more than 70 % of the width of the second bandgap itself. The frequency shift in the first bandgap is 0.43 GHz (30 % of its width).

At the same time, as the air gap width increases within the 0–5 mm range, the amplitudes of Tamm resonances behave differently. In the first bandgap, the amplitudes of reflection and transmission coefficients increase and decrease monotonically, respectively; in the second bandgap, both amplitudes vary non-monotonically in antiphase.

This difference in behavior of the amplitudes of Tamm resonances in the first and second bandgaps is attributable

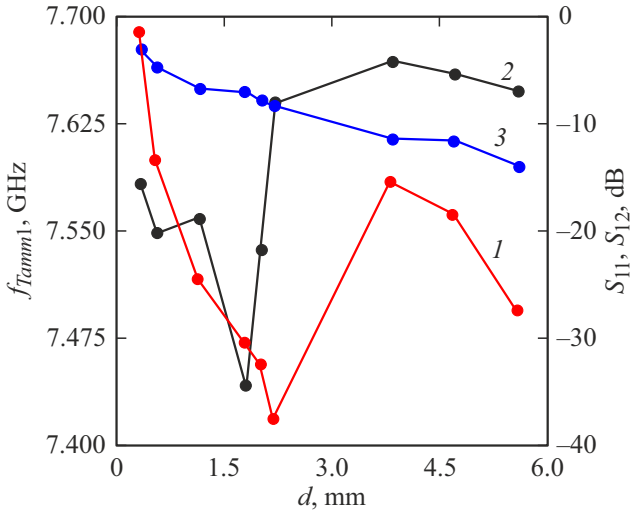

Figure 3. Dependences of frequency f_{Tamm1} (curve *1*) and amplitudes of reflection S_{11} (curve *2*) and transmission S_{12} (curve *3*) coefficients for the Tamm resonance in the first bandgap on thickness of the cellulose paper layer.

to the dissimilarity of dependences of the Tamm resonance frequency on gap size: in the first bandgap, the Tamm resonance approaches the middle level of the bandgap without crossing it, while the resonance in the second bandgap crosses its middle level. When the Tamm resonance shifts towards the middle of either of the two bandgaps, the amplitude of reflection coefficient reaches its maximum, while the amplitude of transmission coefficient reaches its minimum. The gap size at which the Tamm resonance emerges in the middle of the bandgap depends on the thickness of the cellulose paper layer and on the mass fraction of distilled water in it, which sets the value of complex permittivity (Fig. 1).

An Agilent N5242A vector network analyzer was used to measure the amplitude-frequency characteristics of the photonic crystal within the 7–13 GHz frequency range.

The influence of thickness d of the cellulose paper layer with a mass fraction of distilled water of 55 % on the characteristics of the Tamm resonance was examined experimentally (Fig. 3). At small cellulose paper thickness values, the frequency of Tamm resonances decreases in the first (curve *1* in Fig. 3) and second bandgaps with increasing thickness. With thickness $d > 2.2$ mm, the amplitudes of frequency and reflection coefficient (curve *2* in Fig. 3) oscillations decrease in the first bandgap, while the transmission coefficient amplitude (curve *3* in Fig. 3) decreases monotonically at a rate depending on the layer thickness. Similar changes are observed in the second bandgap, but at thickness $d > 1.15$ mm.

A change in the interface structure initiated by introducing an air gap between the photonic crystal and the layer of cellulose paper with a fixed mass fraction of distilled water leads to a change in frequencies of Tamm resonances. In the first bandgap, the shift of the Tamm resonance is less than half the width of the bandgap itself; in the second bandgap, its magnitude is greater than half the bandgap width (curves *1* in Figs. 4, *a* and *b*). Therefore, as follows from the calculation results, the changes in resonance amplitudes are monotonic in the first bandgap (curves *2* and *3* in Fig. 4, *a*) and non-monotonic in the second one (curves *2* and *3* in Fig. 4, *b*).

It should be noted that the non-monotonic variation of amplitudes of the resonances in the second bandgap vanishes at low mass fractions of polar liquid, which correspond to low complex permittivity values.

Thus, the use of cellulose paper with varying mass fractions of distilled water, which is regarded as an element of „green“ electronics with the properties of a microwave energy absorber with controllable parameters, as an interface allows for the emergence of photonic Tamm states in the bandgap. The characteristics of Tamm resonances are controlled by the geometric dimensions and electrophysical properties of cellulose paper and the structure of the interface.

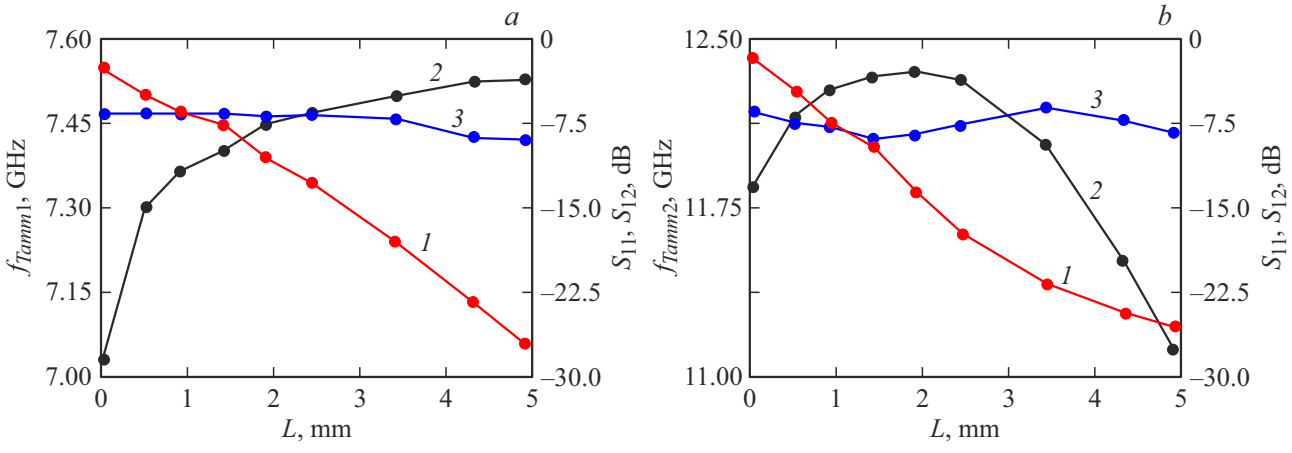

Figure 4. Dependences of frequencies f_{Tamm1} and f_{Tamm2} (curves *1*) and amplitudes of reflection S_{11} (curves *2*) and transmission S_{12} (curves *3*) coefficients for the Tamm resonance in the first (*a*) and second (*b*) bandgaps on gap width.

The obtained results may be applied, e. g., in the design of tunable microwave filters and microwave attenuators based on photonic crystals, where structures based on cellulose paper act as absorbers, and in the characterization of artificial materials based on cellulose and its derivatives with inclusions in the form of polar liquids or conductive nanoinclusions.

Funding

This study was supported financially by grant No. 25-22-00199 from the Russian Science Foundation.

Conflict of interest

The authors declare that they have no conflict of interest.

References

[1] J.T. Orasugh, S.S. Ray, ACS Omega, **8** (9), 8134 (2023). DOI: 10.1021/acsomega.2c05815
[2] Y. Chen, Y. Yang, Y. Xiong, L. Zhang, W. Xu, G. Duan, C. Mei, S. Jiang, Z. Rui, K. Zhang, Nano Today, **38**, 101204 (2021). DOI: 10.1016/j.nantod.2021.101204
[3] S. Li, W. Li, J. Nie, D. Liu, G. Sui, Carbon, **143**, 154 (2019). DOI: 10.1016/j.carbon.2018.11.015
[4] Y.J. Wan, P.L. Zhu, S.H. Yu, R. Sun, C.P. Wong, W.H. Liao, Carbon, **122**, 74 (2017). DOI: 10.1016/j.carbon.2017.06.042
[5] T.W. Lee, S.E. Lee, Y.G. Jeong, Compos. Sci. Technol., **131**, 77 (2016). DOI: 10.1016/j.compscitech.2016.06.003
[6] Z. Zeng, H. Jin, M. Chen, W. Li, L. Zhou, Z. Zhang, Adv. Funct. Mater., **26** (2), 303 (2016). DOI: 10.1002/adfm.201503579
[7] Z. Zeng, M. Chen, Y. Pei, S.I.S. Shahabadi, B. Che, P. Wang, X. Lu, ACS Appl. Mater. Interfaces, **9** (37), 32211 (2017). DOI: 10.1021/acsami.7b07643
[8] S.A. Jose, N. Cowan, M. Davidson, G. Godina, I. Smith, J. Xin, P.L. Menezes, Nanomaterials, **15** (5), 356 (2025). DOI: 10.3390/nano15050356
[9] S. Song, H. Li, P. Liu, X. Peng, Carbohydr. Polym., **287**, 119347 (2022). DOI: 10.1016/j.carbpol.2022.119347
[10] Y. Chen, L. Pang, Y. Li, H. Luo, G. Duan, C. Mei, W. Xu, W. Zhou, K. Liu, S. Jiang, Composites A, **135**, 105960 (2020). DOI: 10.1016/j.compositesa.2020.105960
[11] T.W. Lee, S.E. Lee, Y.G. Jeong, ACS Appl. Mater. Interfaces, **8** (20), 13123 (2016). DOI: 10.1021/acsami.6b02218
[12] L.P. Wu, Y.Z. Li, B.J. Wang, Z.P. Mao, H. Xu, Y. Zhong, L.-P. Zhang, X.-F. Sui, Mater. Des., **159**, 47 (2018). DOI: 10.1016/j.matdes.2018.08.037
[13] J. Wen, Q. Zhao, R. Peng, H. Yao, Y. Qing, J. Yin, Q. Ren, Opt. Mater. Express, **12** (4), 1461 (2022). DOI: 10.1364/ome.455723
[14] Y.J. Yoo, S. Ju, S.Y. Park, Y.J. Kim, J. Bong, T. Lim, K.W. Kim, J.Y. Rhee, Y. Lee, Sci. Rep., **5** (1), 14018 (2015). DOI: 10.1038/srep14018
[15] A.V. Skripal, D.V. Ponomarev, A.A. Komarov, IEEE Trans. Microwave Theory Tech., **68** (12), 5115 (2020). DOI: 10.1109/TMTT.2020.3021412
[16] A.V. Skripal, D.V. Ponomarev, M.A. Volshanik, Tech. Phys. Lett., **50** (8), 26 (2024). DOI: 10.61011/TPL.2024.08.58911.19880.
[17] D.A. Usanov, A.V. Skripal, A.V. Abramov, A.S. Bogolyubov, Tech. Phys., **51** (5), 644 (2006). DOI: 10.1134/S1063784206050173.
[18] S. Fan, M.F. Yanik, Z. Wang, S. Sandhu, M.L. Povinelli, J. Light. Technol., **24** (12), 4493 (2006). DOI: 10.1109/JLT.2006.886061
[19] Al.A. Nikitin, An.A. Nikitin, A.B. Ustinov, E. Lähderanta, B.A. Kalinikos, Tech. Phys., **61** (6), 913 (2016). DOI: 10.1134/S106378421606013X.
[20] https://www.cmc.ca/wp-content/uploads/2019/08/Basics_Of_MeasuringDielectrics_5989-2589EN.pdf

Translated by D.Safin